Title: On the reproductive mechanisms of protocells

Dheeraj Kanaparthi[1,2&3*], Marko Lampe[4], Jan-Hagen Krohn[1&3], Falk Hildebrand[5], Thomas Boesen[6], Andreas Klingl[7], Prasad Phapale[8], & Tillmann Lueders[2&3*]

Affiliations:

[1]Department of Cellular and Molecular Biophysics, Max-Planck Institute for Biochemistry, Munich, Germany.

[2]Chair of Ecological Microbiology, BayCeer, University of Bayreuth, Germany.

[3]Excellenzcluster ORIGINS, Garching, Germany.

[4]Advanced Light Microscopy Facility, European Molecular Biology Laboratory, Heidelberg, Germany.

[5]Quadrum institute, Norwich, UK.

[6]Department of Biosciences, Center for Electromicrobiology, Aarhus, Denmark.

[7]Department of Biology, LMU, Planegg-Martinsried, Germany.

[8]European Molecular Biology Laboratory, Heidelberg, Germany.

Abstract: The most primitive cells or protocells were thought to be devoid of all complex molecular biological processes. They are believed to have mediated cellular processes like reproduction entirely by biophysical properties of cell constituents and fluctuating environmental conditions. Despite these propositions, a complex biological process like reproduction has never been shown to be mediated entirely by environmental conditions. To understand the reproductive process of protocells in their native habitat, here we used a top-down approach to transform bacterial cells into a primitive lipid vesicle like-state in which cells are devoid of all molecular biological mechanisms regulating their reproduction. We then grew these cells under the environmental conditions of early Earth, to understand if and how these cells reproduce. Despite the loss of innate ability to regulate reproduction, cells in our experiments underwent reproduction always yielding viable daughter cells. The lifecycle and fission of parent cell into multiple daughter cells can be explained by interaction between intracellular metabolism, physicochemical properties of cell constituents and environmental conditions. Based on our observations we argue that reproduction is an inherent property of cells with an internal metabolism, without a need for dedicated molecular biological processes, albeit at a reduced reproductive efficiency.

Key words: protocells, Gram-positive protocells, protocell reproduction, membrane biophysics, membrane phase-separation, cell-division, chemical evolution.

The theory of chemical evolution proposes that prokaryotes evolved from more primitive protocells[1]. These cells were hypothesized to be primitive and devoid of all complex molecular biological processes. This led to the proposition that processes like reproduction in these cells had to be mediated entirely by physicochemical properties of their cell constituents[2]. Given the hypothesised simplicity of these cells, lipid vesicles (LVs) with an

aqueous core are widely used as proxy-protocells[2–4]. Most of our current understanding and theories about protocells are largely a result of studying such LVs. Despite accomplishing considerable progress in our understanding of protocells, we believe LVs do not represent the true complexity of protocell.

To replicate the complexity of a protocell, here we worked with protoplasts of Gram-positive bacteria as proxy-protocells (*Exiguobacterium strain M* protoplasts –*EM-P*). Our choice of using bacterial protoplasts is based on three key considerations. First, protocells like the bacterial protoplasts were most likely devoid of a peptidoglycan cell wall. Synthesis of cell wall components, transporting of monomers across the cell membrane and their subsequent assembly into a peptidoglycan cell wall is a physiologically complex process requiring multitude of enzymes working in co-ordination with one other[5,6]. Evolutionarily primitive protocells most certainly were devoid of such complex molecular biological processes. Second, like the protocells, protoplast lack an innate ability to regulate either their morphology or mediate reproduction[7–9]. They can be described as simple bag of cytoplasm reproducing in a haphazard manner[10]. Third, even the most primitive self-replicating life forms like the protocells must have possessed physiological mechanisms for energy conservation used for building their biomass, genetic material for encoding information for these processes and a means of reproduction yielding viable daughter cells. Even these fundamental processes require considerable cytoplasmic complexity. The cytoplasm of such a protocell most likely resembled a bacterial cytoplasm in its physicochemical properties, rather than an aqueous core of a LVs. Given these similarities we argue that bacterial protoplasts better simulate protocells rather than LVs.

Apart from the cytoplasmic composition, physicochemical properties of the cell constituents are known to be determined by the environmental conditions[11,12]. Hence, we believe any attempt to understand protocell reproduction, should be conducted in their natural habitat. To achieve this objective, we grew *EM-P* under the environmental conditions of early Earth. Recent geological studies suggests that Earth's surface had cooled enough to accommodate liquid water during the Hadean Eon[13] creating environmental conditions conducive for the emergence life[14]. The earliest unambiguous evidence of life exhibiting complex CO_2 fixation pathways dates to 3.8 billion years ago (early Archaean Eon)[15,16]. This constrains the entire process of chemical evolution to the Hadean Eon and the first appearance primitive protocells most like to late Hadean or early Archaean Eon[17]. The exact environmental conditions of Archaean Earth are currently unclear. Nevertheless, an emerging consensus among the scientific community suggests that at least by 3.8 billion years ago surface temperatures likely ranged between 26° to 35°C[18,19]. Early Earth's ocean are also hypothesized to be 1.5 to 2 times saltier than the present-day oceans[20]. To replicate these conditions, we grew *EM-P* in half-strength tryptic soy broth amended with 5-8% (w/v) Dead Sea salt (TSB-DSS) at 30°C. We used DSS, rather than pure NaCl was used in our experiments to better simulate the complex salt compositions of natural environments. We then monitored these cells at regular intervals using super-resolution microscopy to understand if and how these cells grow and reproduce.

In the following sections of the manuscript, we present the lifecycle of *EM-P* under Archaean Eon environmental conditions. We also present an in-depth comparison between the reproductive processes observed in our study to previous studies on LVs, to provide a mechanistic explanation of the observed processes. Our results show that cells can undergo division and form live daughter cells, even when reproduction is not being coordinated by

molecular biological processes. The mechanism of their reproduction can be explained by the physicochemical properties of the cell constituents and environmental conditions.

Results & Discussion

Rather than reproducing in a haphazard manner[10], cells in our incubations reproduced in a defined sequence of steps. During the early growth stages, *EM-P* reproduced either by budding or by binary fission (Movies S1-S3). In the subsequent growth stages, *EM-P* was observed to be reproducing by two different processes. In brief, it either reproduced by the forming external or internal daughter cells. Sequential steps involved in reproduction by formation of external and internal daughter cells are shown in Movies S4-S11 and Movies S12-S18 respectively.

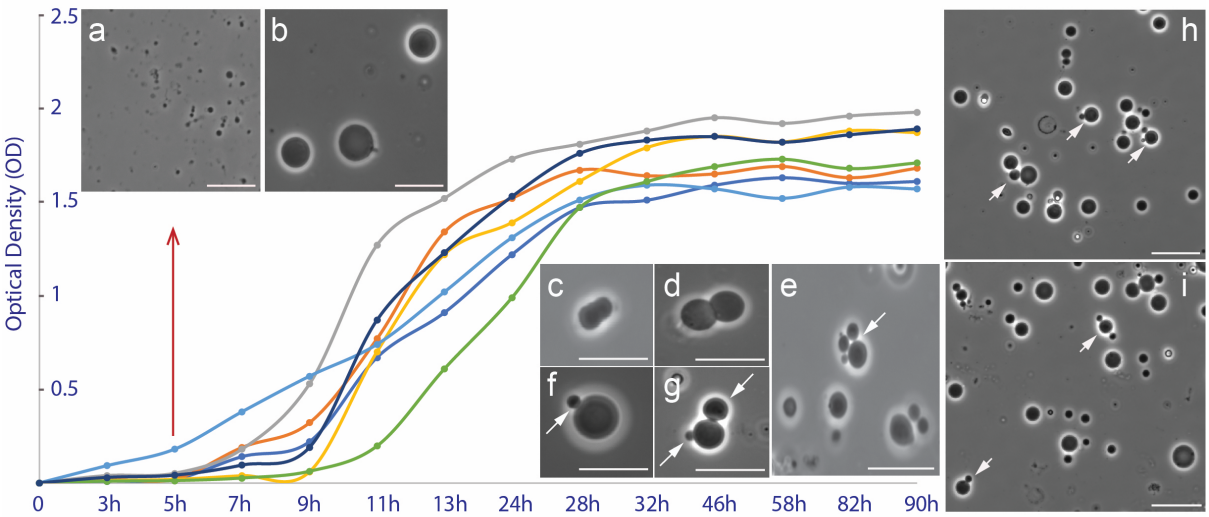

Figure 1. Growth characteristics of *EM-P* in batch culture. *EM-P* exhibited a typical sigmoid growth curve with an initial phase of slow growth rate (lag phase), a log phase with exponentially increasing cell numbers and a gradual decline in the growth rate during the stationary phase. The X and Y-axis in the plot indicate the time in hours (h) and optical

density. Images a & b shows typical morphologies of cells in early and late lag-phase (notice an increase in the size of the cells). Images c-i, show early log phase cells that seems to be reproducing either by binary fission (c, d and Movie S2 & S3) or budding (arrows). Images f – i show variation in the sizes of the daughter cells (buds). Scale bars: 10μm.

During the lag and early-log growth phase, *EM-P* gradually grew by an order of magnitude in size (Figure 1a, b & Movie S1). Apart from growing in volume, cells in this growth stage were in a constant state of surface deformations (Movie S1-S3). Subsequently, these spherical cells then transformed into ovoid shapes (Figure 1c & Movie S2). They then developed surface invaginations (Figure 1c, d & Movie S2), which gradually got deeper, transforming an oval-shaped cell into two distinct daughter cells (Figure 1d & Movie S3). These cells subsequently underwent fission, resulting in individual daughter cells. A similar case of surface instability followed by coalescence into distinct cells and subsequent fission was reported earlies in droplets[21,22] and LVs[23]. In these studies, the surface instability and subsequent fission into daughter cells was directly linked to the either to the physical activity within the vesicles/droplets like Brownian motion or changes in the environmental conditions[21,22]. Given that *EM-P* is physiologically active with intracellular metabolism, we propose that metabolic reactions within the cell or the interaction between intracellular components and membrane could have resulted in the surface undulations and subsequent fission of the cells[22].

We occasionally saw cells undergoing fission but still connected by a narrow membrane tether (Movie S3). Despite having the appearance of binary fission, no uniformity was observed in the sizes of the daughter cells (Figure 1d-i). Depending on the size of the daughter cells, cells in this growth stage appear to be reproducing either by budding or by

binary fission (Figure 1c-f, S1 & Movies S1-S3). This lack of uniformity in size and number of daughter cells formed from a single parent *EM-P* is likely explained by heterogenous spontaneous curvature of membrane components[24]. Most previous studies attempting to understand the biophysical properties of protocells were conducted on LVs of simple chemical composition. In such studies, the physical properties of membranes like elasticity and spontaneous curvature along their surface remain largely homogeneous. Unlike the LVs, cell membranes are composed of diverse lipids species and intercalated by proteins. The formation of lipid-lipid[25] and lipid-protein[26] complexes results in the formation of nanodomains with different physical properties and spontaneous curvature, leading to lateral heterogenicity in the physical properties of cell membranes[24]. Theoretical models attempting to understand fission in LVs with such heterogenous membranes proposed that they undergo asymmetric fission and form daughter cells of different sizes (Figure 2a&b), very similar to what we observed in *EM-P* (Figure 2). Given these similarities between theoretically predicted morphologies and *EM-P*, we propose that lateral heterogeneities in the physical properties of the plasma membrane due to its compositional complexity could have resulted in an asymmetric cell division in *EM-P* (Figure 2).

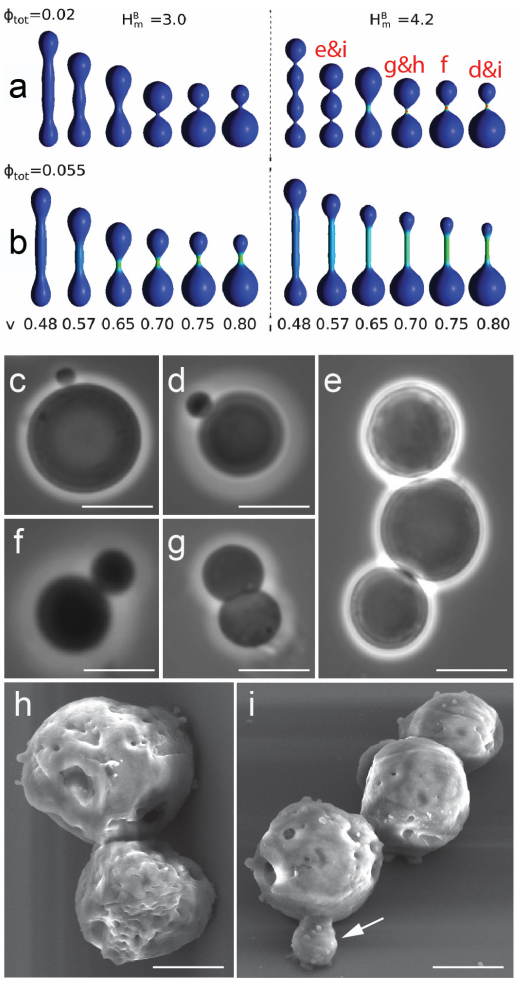

Figure 2. Asymmetric division of *EM-P* during log-phase. Images a & b show theoretical morphologies of vesicles with curvature heterogenous membrane[24]. v is the ratio between the actual volume of a vesicle to the volume of a spherical vesicle with the same surface area, Φ_{tot} – is the concentration of the curved membrane component, H^B_m – is its intrinsic curvature (originally published by Bobrovska *et al*., 2013)[24]. Images c-i show, phase-contrast (c-e) and SEM (h&i) images of *EM-P* cells undergoing a similar method of reproduction. Scale bars: 10µm (c-e) & 2µm (h&i).

During the late log-phase, most cells were observed to have formed hollow filamentous or spherical extensions, extending either out of the cell or into the cell as intracellular vesicles (Figure 3, 4, Movies S4 & S12). Formation of these structures can be explained by the biophysical properties of its cell constituents and an unorderly molecular biological

regulatory mechanism[7]. Apart from reproducing independent of canonical processes[7,27], protoplasts also differ from their walled counterparts in terms of their excessive lipid synthesis[8]. This excessive lipid synthesis in protoplasts results in a cell state where the surface area of the cell membrane far exceeds its cytoplasmic volume. When a similar state is induced in LVs by the application of osmotic stress, vesicles are known to undergo shrinkage in a sequence of steps involving the formation of buds and filamentous extensions[28,29]. Morphological transformation of *EM-P* observed in our study was very similar to vesicle undergoing osmotic shrinkage[12,30]. Like the LVs, morphologies of *EM-P* can be explained by the rate of cytoplasmic volume increase (i.e., its growth rate), expansion strain on the membrane surface, and the amount of excess membrane.

The absence of filamentous extensions during the early log phase (Figure 1) and their appearance during the late log phase (Figure 4) can be explained by the differences in the rate of cytoplasmic volume increase and the rate of lipid synthesis during different growth stages. In the early log phase, cells were in a state of rapid growth. In this growth stage, the rate of cytoplasmic volume increases kept pace with lipid synthesis. Hence, cells in the early log phase were largely devoid of hollow membrane extensions (Figure 1). With a gradual reduction of growth rate towards the late log phase, the rate of membrane synthesis far exceeded the rate of cytoplasm volume increase. This imbalance between the cell volume and surface area of the plasma membrane, could have led to the formation of hollow membrane extensions (Figure 2&3) as a mechanism of accommodating the excess membrane[30]. In support of this observation, *EM-P* did not develop filamentous extensions when they were kept in a constant state of logarithmic growth by transferring them into fresh media every few hours. These observations suggest that the growth rate (*i.e.,* rate of cytoplasm volume increase) has a direct influence on the morphology of the cells.

Formation of external and inter membrane structures can also be explained by the model proposed by Lipowsky & Jülicher[31,32]. It was proposed that phase-separated membranes tend to minimize interfacial energy at the phase boundary to attain a thermodynamically stable state. They do so by forming an out-of-plane membrane invagination, which gradually transforms the softer liquid disordered (L_d) membrane into a bud (Figure 3). Earlier studies hypothesized that L_d membrane most likely undergoes budding due to its low bending rigidities and high spontaneous curvature[30]. Despite these propositions[25], to date membrane phase-separation has only been reported in LVs. To the best of our knowledge, ours is the first study to provide visual evidence of membrane phase-separation in live cells (Figure 3)[33]. In accordance with this theory[25], the cell membrane underwent phase-separation into L_d and L_o membrane (Figure 3). L_d membrane initially appeared as small patches on the cell surface, less than 180nm in diameter (Figure 3a-c). As the area of L_d membrane increased, it underwent budding due to an increase in the line tension at the phase-boundary[34] (Figure 3g, h & Movie S18). Nevertheless, some deviations from this expected behavior were observed. First, there was the difference in the direction of budding. Contrary to the predictions, we observed L_d-membrane undergoing a negative (into the cell), rather than positive (out of the cell) curvature (Figure 3g). Second, despite its higher bending rigidity, liquid-ordered (L_o) membrane too underwent deformation out of the cell (Figure 3d-f, arrows 3g, cell within the highlighted region & Movie S18). Intriguingly, all positive (out of the cell) membrane deformations were exclusively composed of L_o-membrane and all negative membrane deformations (into the cell) were exclusively composed of L_d-membrane (Figure 3 & Movie S18).

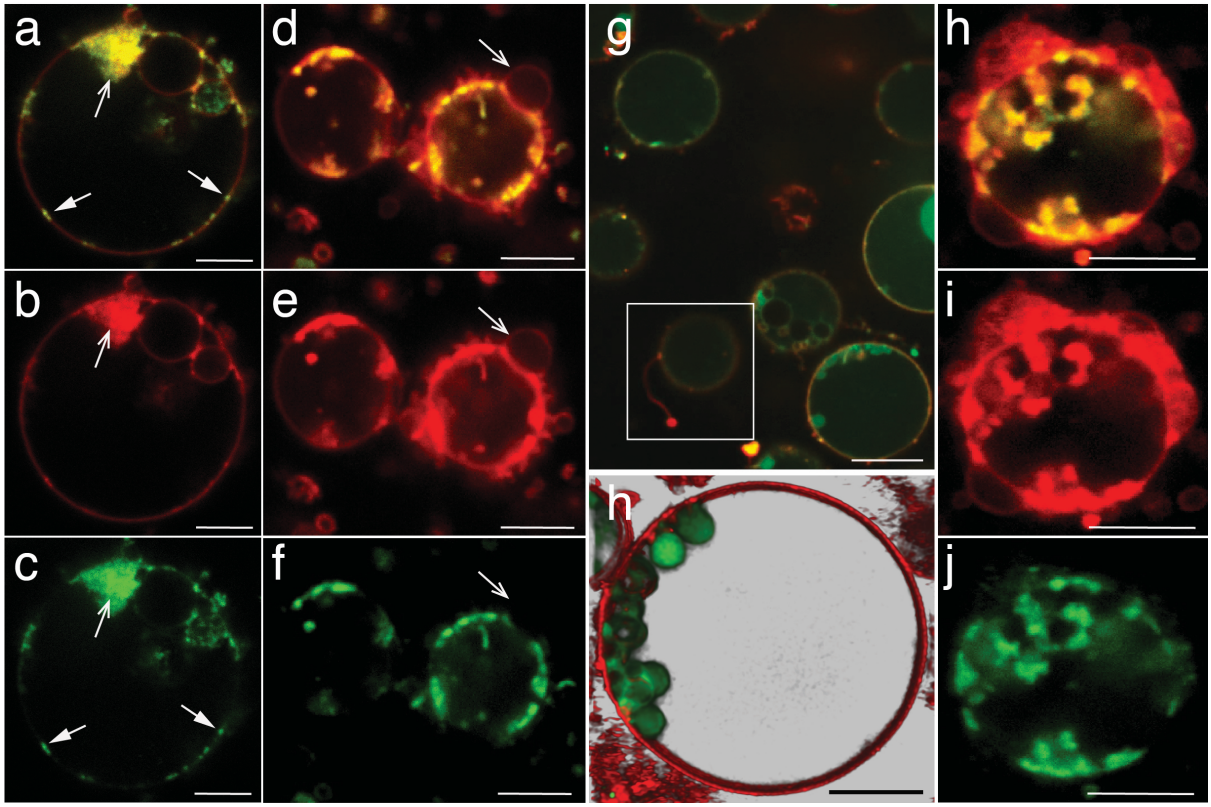

Figure 3. Membrane phase-separation in *EM-P*. Cells in these images were stained with FM™5-95 (all membrane, red) and *FAST*™ DiI (L_d-membrane, green) and imaged either using a spinning disk confocal (g & h) or a super-resolution, STED microscope. Images a-c, d-f and h-j are different channels of the same *EM-P* cell. Closed arrow in a-c: small patches of L_d-membrane (≈ 180nm) on the cell surface. Open arrows in a-c: large clumps of coalesced L_d-membrane within the cell. Similar aggregations of L_d-membrane can also be seen in images d-f and h-j. Open arrows in d-e: L_o-membrane undergoing positive membrane curvature. Image g show *EM-P* cells with filamentous extensions entirely composed of L_o membrane (Movie S18). Image h show 3D-rendered image of an *EM-P* cell exhibiting membrane phase separation. A series of optical sections of the stacks shown in Figure S1. Scale bars: 10µm (a-f & h-j) & 5µm (g & h).

The direction and physical nature of a membrane undergoing budding could be explained by its lipid composition, bi-layer asymmetry, the concentration of sterols, and the nature of the

aqueous core. Bacia *et al.* studied the influence of cholesterol and related sterols on budding[35]. Despite higher bending rigidities, this study showed that some sterols can induce the budding of L_o membrane instead of L_d membrane. Prokaryotes are known to lack sterols like cholesterol and its derivatives, but are known to possess functional analogues of cholesterol, like hopanoids[36]. The properties of these compounds in inducing membrane phase separation and budding were rarely investigated. Apart from sterols, invagination of more rigid L_o membrane was also reported to happen when LVs[28] experience a state of excess membrane (like during the osmotic shrinkage), possibly due to an increase in the spontaneous curvature of L_o membrane[30]. The nature and direction of the membrane invagination could also have been determined by the aqueous core (cytoplasm) and media surrounding the cell[37]. Studies showed when liquid-liquid phase-separation was induced in the aqueous core (not the membrane) of a LVs the vesicle membrane too undergo phase separation according to their densities[30,38]. The denser phase of the aqueous core was observed to have been associated with L_d membrane and the lighter phase with L_o membrane[37]. This could explain the invagination of L_d membrane into the cell, given the higher densities of cytoplasm (~17-35 wt% molecules). Preference of L_o membrane to the comparatively less dense growth media (~6-7 wt% molecules), could have led to L_o membrane undergoing positive curvature *i.e.,* out of the cell (Figure 3 & Movie S20).

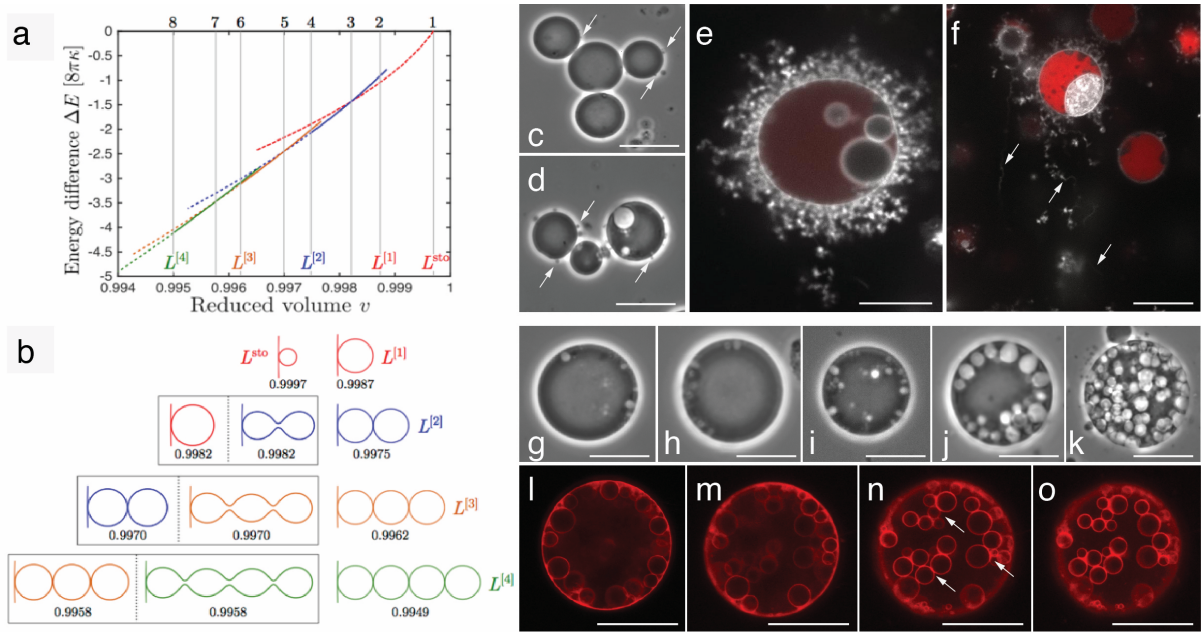

Figure 4. Comparison between theoretically predicted steps in filament formation to observation in *EM-P*. Images a & b were originally published by Liu *et al.,* 2015[30]. Image A show energy landscape of different equilibrium shapes as a function of reduced volume (v). ΔE indicates deflation induced reduction in bending energy. Image b shows the shapes of filamentous extensions corresponding to eight vertical lines in image a. Images c-o show images of *EM-P* cells from different growth stages with external (c-f) or internal membrane (g-o) structures that were formed in a pattern similar to what was theoretically predicted (a & b). Arrows in images c & d points to late-log phase *EM-P* cells with tiny membrane extensions. Image E show cells surface covered with short filamentous extensions. Image f show cells stationary growth stage cells with longer filamentous extensions. Cells in these images were stained with universal membrane stain, FM™5-95 (white) and DNA stain, PicoGreen™ (red). Images g-k show sequential stages observed in the development of intracellular vesicles. l-o show optical sections of a Nile red stained *EM-P* cell at different planes. Arrows in these images points to interconnected nature of these vesicles similar to $L^{(3)}$ and $L^{(4)}$ in image b. Scale bars: 10µm.

The formation of external membrane extensions during the late log phase happened in a series of steps (Figure 4). Cells first formed hollow buds-like structures from multiple locations on the cell surface (Figure 4c&d). In the subsequent growth stages, these buds transformed into short filamentous extensions, often covering the entire surface of the cell (Figure 4e, 5b & Movie S19). These filamentous extensions gradually increased in length (Figure 4f). This sequence of formation and transformation of filamentous extensions was reported previously in LVs[30]. In case of LVs, formation of filamentous extensions depends on the osmolarity of the media and rate of osmotic shrinkage. Slow transfer of lipid from the parent cell into these filamentous extensions[30], led to the formation of shorter membrane extensions from multiple sites on the cell surface. A relatively faster rate of lipid transfer, led to the extension of already formed filaments rather than forming new filaments. In case of *EM-P,* we argue that rate of lipid transfer is dependent on its growth kinetics. During the log phase when the growth rate is high, cytoplasmic volume increase kept pace with the membrane synthesis i.e., less membrane was available for formation of hollow filamentous extensions. Hence during this growth stage, formation of small surface invaginations at multiple sites is favored (Figure 4c&d). During the later growth-stage, when the ratio of cytoplasmic volume increase to amount of excess membrane is low i.e., more membrane area is available for the formation of hollow filamentous extensions. Under such conditions, it is energetically favorable for already existing filamentous structures increase in length (Figure 4f), rather than forming new membrane invaginations on its surface.

In the subsequent growth stages filamentous extensions grew in volume by the transfer of cytoplasm from the parent cell (Figure 5). During this process, these filamentous extensions developed surface depressions along their length, reminiscent of tubular vesicles subjected to

curvature-induced destabilization at their surface (like Rayleigh-Plateau instability) (Figure 5). This led to the transformation of the filaments from a tubular into a "string-of-beads" morphology (Figure 5c-e). Following the transfer of cytoplasm, these extracellular filaments detached from the parent cell and fragmented into individual daughter cells in a sequence of steps as shown in Figure 5d-g (Movies S11).

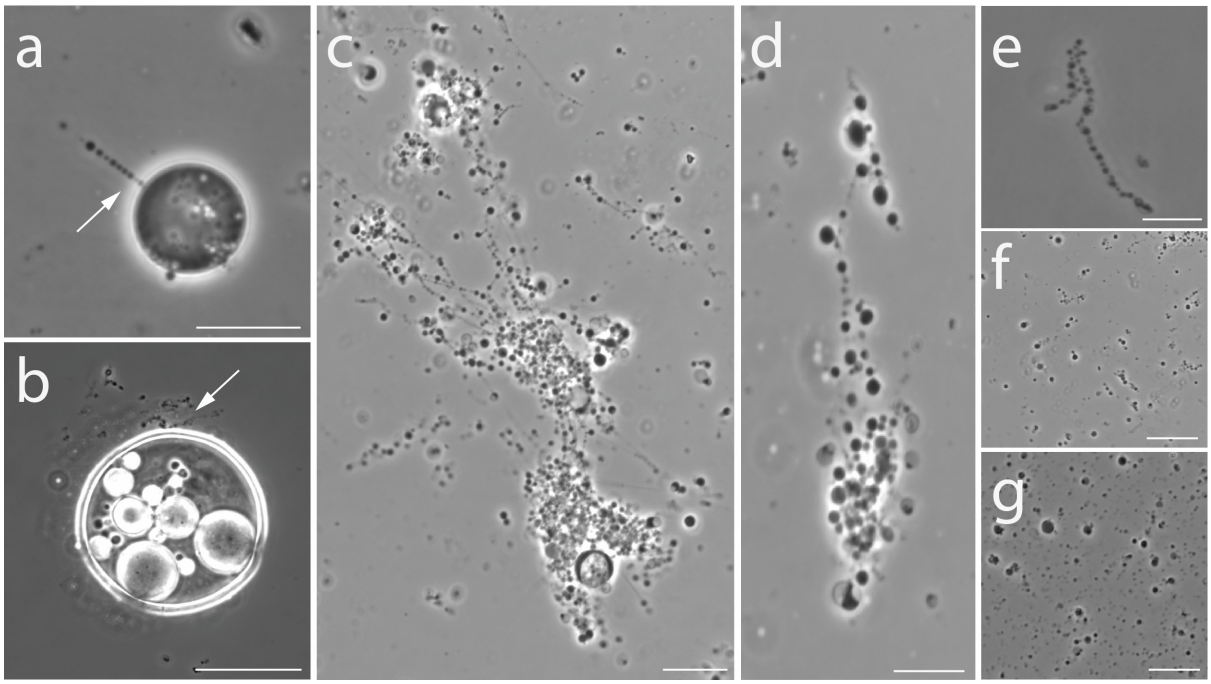

Figure 5. Life cycle of *EM-P* reproducing via formation of extracellular daughter cells. Image a show a late log phase cell with filamentous (arrow) membrane extensions. Image b shows a cell from a subsequent growth stage cells with multiple filamentous extensions. Images c-g show formation of daughter cells as string-of-beads, detachment of these strings of daughter cells and their subsequent fragmentation into individual daughter cells. Also shown as Movies S11. Scale bars: 10μm (a-g).

This transformation of hollow tubular vesicles into string-of-spherical daughter cells could be explained by two different mechanisms. One could have been the spontaneous transformation of tubular vesicles into a string-of-beads morphology to reduce the interfacial area to reach a

thermodynamically stable lower energy state[38]. A similar transformation of filamentous structures was reported previously in LVs, especially the one undergoing osmotic shrinkage[38,39]. This inherent tendency of tubular vesicles to spontaneously deform into a "string-of-beads" morphology could have led to the formation of spherical daughter cells (Figure 5a-c). Alternately, formation of daughter cells could also be explained simply by the lower volume of cytoplasm that was transferred into the filaments compared to the total volume of the filament[30]. The excess membrane within these tubular structures should have collapsed and transformed into tethers connecting adjacent daughter cells (Figure 5c&d).

The formation of hollow internal vesicles followed a trend similar to what we observed for external filamentous extensions (Figure 4g-o & Movie S11). At first, multiple tiny intracellular vesicles filled with growth media appeared along the cell surface (Figure 4g&h). They were formed by a process resembling endocytosis (Figure 6a, white arrows). In the subsequent stages, these vesicles increased in volume (Figure 4j). In some *EM-P* cell vesicles constituted a large fraction of intracellular volume (Figure 6c & S2), with cytoplasm restricted to narrow spaces in-between the hollow vesicles (Figure S2 & Movie S12). We also observed a second method of intracellular vesicle formation (Figure S3 & S4). In this process, excess membrane initially accumulated as folded lump attached to the membrane surface (Figure S3a-d & S4). With the influx of growth media, these lumps expanded into a large individual vesicle or into a string of vesicles (Figure S3c-i). Cells in this growth stage are morphologically diverse with multiple spherical, filamentous (Figure S3 & S5) or intracellular vesicles interconnected by filamentous strings (Figure S3).

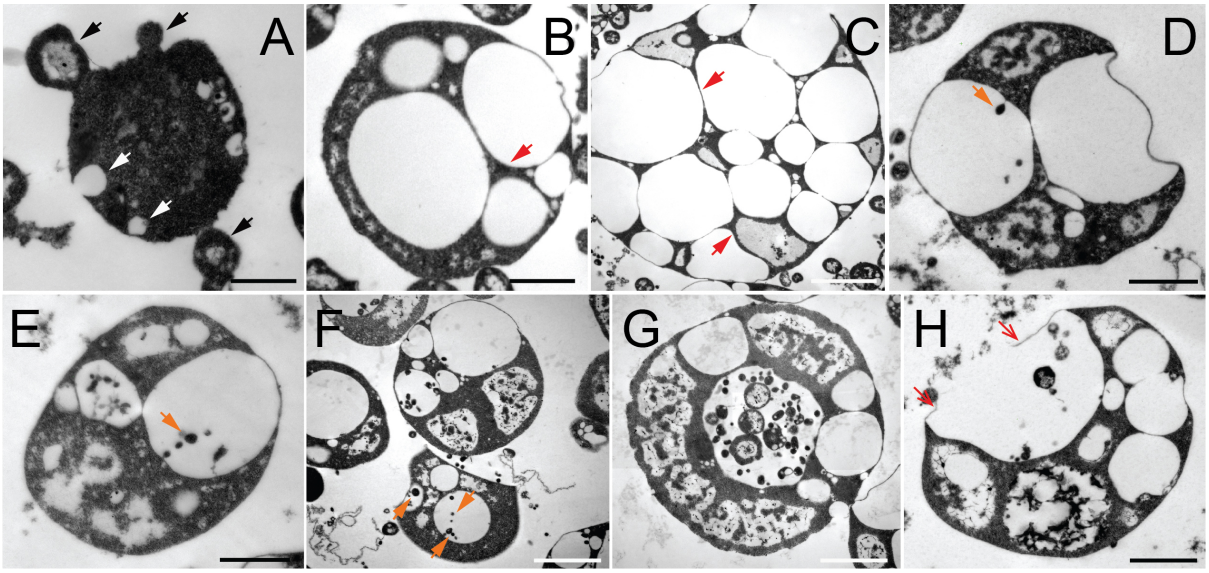

Figure 6. The life cycle of *EM-P* reproducing via formation of intracellular daughter cells. Images a-h are TEM images of the life cycle of *EM-P* reproducing by the formation of intracellular daughter cells. Image a show the process by which intracellular (white arrows) vesicles and bud-like structures are formed (black arrows). Closed red arrows in images b & c points to the narrow cytoplasmic region of the cell. Arrows in images d-f points to the formation of individual and string of daughter cells or string of multiple daughter cells. Image g show internal daughter cells with intracellular vesicles. Image h shows the process of daughter cell release by rupture of vesicle membrane (open red arrows). Scale bars: 1μm.

After the formation of intracellular vesicles, the vesicle membrane then underwent a positive curvature to form bud-like structures extending into the vesicles (Figure 6d, orange arrow). Multiple such structures were observed within a single vesicle originating from different points (Movie S12). These buds either detached from the vesicle surface as individual daughter cells (Figure 6e-g) or grew into a string of multiple daughter cells (Figure 6e, orange arrow & Movie S13), which then fragmented into individual daughter cells (Figure 6g, S6 & Movie S9 & S16).

Strings of both external and internal daughter cells detached from the parent cells by the rupture of membrane tethers (Figure 5c-g, 6e-g & Movie S9-S11). They subsequently fragmented into individual daughter cells (Figure 5c-g, 6e-g & Movie S9-S11). Individual daughter cells had been formed into the intracellular vesicle, were released into the surrounding media either by one-step rupture of the cell membrane (Figure 6h) or by a two-step process (Figure S7) of cell membrane lysis to release intracellular vesicles (Movies S14-S16). Followed by the vesicle membrane lysis releasing the daughter cells (Movies S18). Daughter cells formed by this process were tiny (0.2 - 1μm in diameter) in comparison to the parent cells (Figure 6g, 6h & S17) and are highly mobile (Movie S8-S10 & S17). Due to the gradual transfer of cytoplasm from parent to daughter cells, after 2-4 days of growth most *EM-P* cells were depleted in their cytoplasmic content (Figure S6). After 2-3 days of growth, batch cultures of *EM-P* largely consisted of cells with all the above-described morphologies along with a considerable amount of membrane debris (Figure S8).

One key aspect of the cell-cycle is the fission of the parent cell into metabolically viable daughter cells. Achieving fission among LVs has been the primary focus of multiple studies and is of key importance in enhancing our understanding of the most primitive cell replication processes[40] and building autonomously replicating synthetic cells[41,42]. Previous studies achieved fission by mechanical means[43] or by encapsulating protein involved in cell division into LVs[44] or by constant incorporation of fresh lipids into the LVs[2]. Given that *EM-P* was grown under static conditions and has ineffective molecular biological regulatory processes[7], we presume that the forces driving the fission process were intrinsic to the cell and primarily biophysical in nature. During all the growth stages we observed that cells were in a constant state of surface undulations (Movie S1-S3 & S9-S11). We presume these constant deformations at the cell surface could have provided the force required for the

fission of a parent cell into two daughter cells (Movies S9-S11) or fragmentation of string-of-daughter cells into individual cells. These surface deformations were a result of differences in osmolarities[45], chemical composition (organic carbon within the cell and salts outside the cell) or concentrations of different compounds on either side of the membrane[12]. All these factors together with the virtue of processing an internal metabolism[22] were hypothesized to generate surface deformations, ultimately leading to cell fission. We also observed movement of intracellular constituents within *EM-P* (Movie S21), which could also have contributed to surface deformations. We do not presume that proteins involved in canonical cell replication resulted in surface undulations. Treatment of *EM-P* with bactericidal chemicals like sodium azide (0.3%)[46] or protein polymerizing agents like 0.5% glutaraldehyde and formaldehyde[47] inhibited growth which did not recover when transferred into fresh media. However, treatment of cells with these chemicals did not result in a static cell, devoid of surface deformations. These surface deformations could only be halted by equilibrating cytoplasmic components with the outside by creating pores in the membrane using Triton X100 (0.5%)[47]. These observations supports our hypothesis that asymmetric conditions on either side of the cell membrane or Brownian motion of intracellular constituents (Movie S21) caused the surface deformations[48], rather than the action of specific proteins[44]. A similar case of surface deformations causing the fission of cells was shown by earlier studies both in droplets[22] and LVs[44,48].

In an attempt to understand the reproductive processes of protocells in its natural habitat we grew *EM-P* in a hyper-saline media of complex salt composition. It is a well-established fact that different cations interact differently with cell membrane and alter their physical properties[11,12,49]. To understand how individual components of DSS influenced the morphology and life cycle of *EM-P*, we replaced DSS in the growth media with equivalent

concentration of individual salts like KCl and $MgCl_2$ (5%w/v). When grown in TSB-5%KCl, cells reproduced predominantly via formation of intracellular daughter cells (Figure S7). Cells in these incubations are larger than cells grown in DSS (Figure S7). In sharp contrast, cells grown in TSB-5%$MgCl_2$ were significantly smaller in sizes in comparison to cells grown in equivalent concentrations of DSS or KCl (Figure S8). The diameter of these cells was restricted to 0.5-2μm and reproduced by forming extracellular daughter cells (Figure S8). These differences can be explained by the nature of interactions between cations and phospholipid head groups[12]. Earlier studies reported that monovalent cations like potassium increases the fluidity of the membrane, whereas divalent cations like magnesium decrease the fluidity[11]. This increase in membrane fluidity could have facilitated expansion of cells in incubations contain DSS and KCl[12] resulting in relatively larger cells. Reduced elasticity of the membrane in the presence of $MgCl_2$ could have led to the formation of smaller cells (Figure S8). The reasons for the reproduction predominantly via extracellular daughter in the presence of $MgCl_2$ and predominantly via intracellular daughter cells in the presence of KCl are currently unclear. Nevertheless, a similar phenomenon of intracellular vesicle formation in the presence of KCl was observed previously in LVs[12]. *EM-P* reversibly change its morphology when transferred between media of different salt compositions. This suggests that chemical composition of the growth media, rather than the information encoded in its genome influenced the morphology of *EM-P*.

Unlike the growth conditions used in our experiments, cells within the natural environments are rarely static. Most cells in natural environments especially the cells inhibiting early Earth were likely subjected to constant agitation by wave action. To understand the influence of such physical forces on *EM-P*'s morphology and reproductive processes, we grew *EM-P* on an orbital shaker. Under these growth conditions, *EM-P* reproduced exclusively by a process

resembling binary fission, similar to the cells in the early log phase (Figure 1c-i). None of the above-described morphologies like large cells with intracellular vesicles, and strings of daughter cells were observed. To the best of our knowledge ours is the first study to report such a profound influence of environmental conditions on the life cycle of bacterial cells.

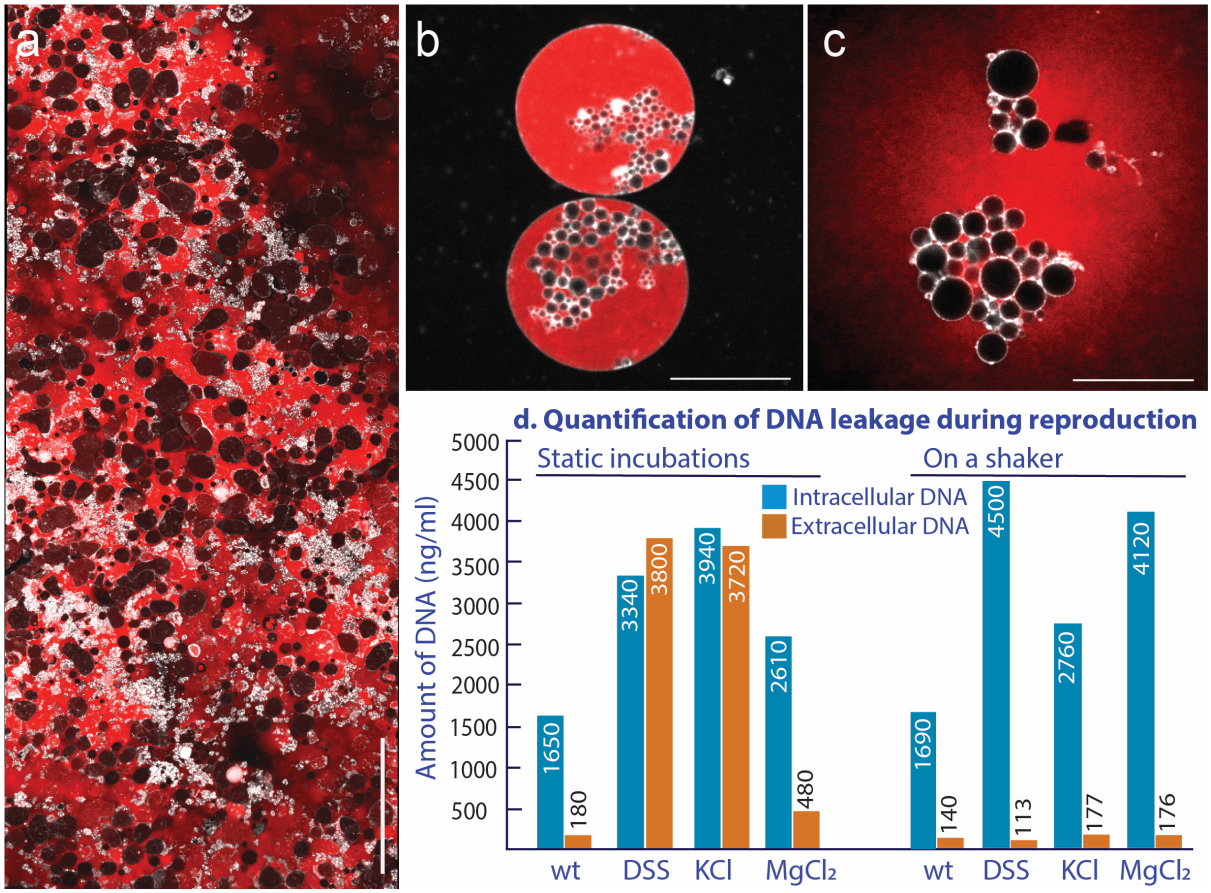

Figure 7. Leakage of cell constituents during *EM-P*'s reproduction. Images a-c shows *EM-P* cells during early (b) and late log growth stages (a). Cells in these images were stained with FM^{TM}5-95 (membrane, white) and PicoGreen^{TM} (DNA, red) and imaged using a STED microscope. Image c show lysis of cells and release of intracellular constituents. Scale bars: 10µm. Image d show the amount of intracellular and extracellular DNA during the late log growth stage (Figure S10, for all growth stages). wt – wild type (*Exiguobacterium strain M*

with a cell wall); DSS, KCl & $MgCl_2$ - *EM-P* grown in TSB amended with 6% of the respective salts.

Considerable amount of membrane debris (Figure S8) and extracellular DNA were observed in our incubations during all growth stages (Figure 7 & S10). These observations imply that, *EM-P's* method of reproduction is leaky resulting in significant loss of intracellular constituents. DNA could have been released into the surroundings when cell underwent lysis to release daughter cell (Figure 6h, S5 & Movies S15-S18) or was a result of cells undergoing explosive lysis during all growth stages (Figure S11 & Movie S22). To the best of our knowledge, such explosion of bacterial cells was not reported previously. However, similar rupture of LVs by two different mechanisms was previously known. Lysis of cells may have been caused due to osmotic pressure created by Reactive Oxygen Species (ROS)[50] or by interactions between DNA and lipid head groups[51]. ROS-induced lysis of cells could also have been photo-induced during the imaging process (by confocal or a STED microscope). Nevertheless, we observed end products of cell lysis when cells were incubated in dark and imaged using a phase-contrast microscope at fewer intervals (48h – 72h). Hence, we consider lysis to be a natural part of *EM-P*'s cell-cycle, rather than an artifact of the imaging process. In fact, bacterial protoplasts are known to produce high amount of ROS[27]. Hence, there exists a possibility that lysis observed in *EM-P* could have been induced by ROS by interactions between DNA and the cell membrane[51].

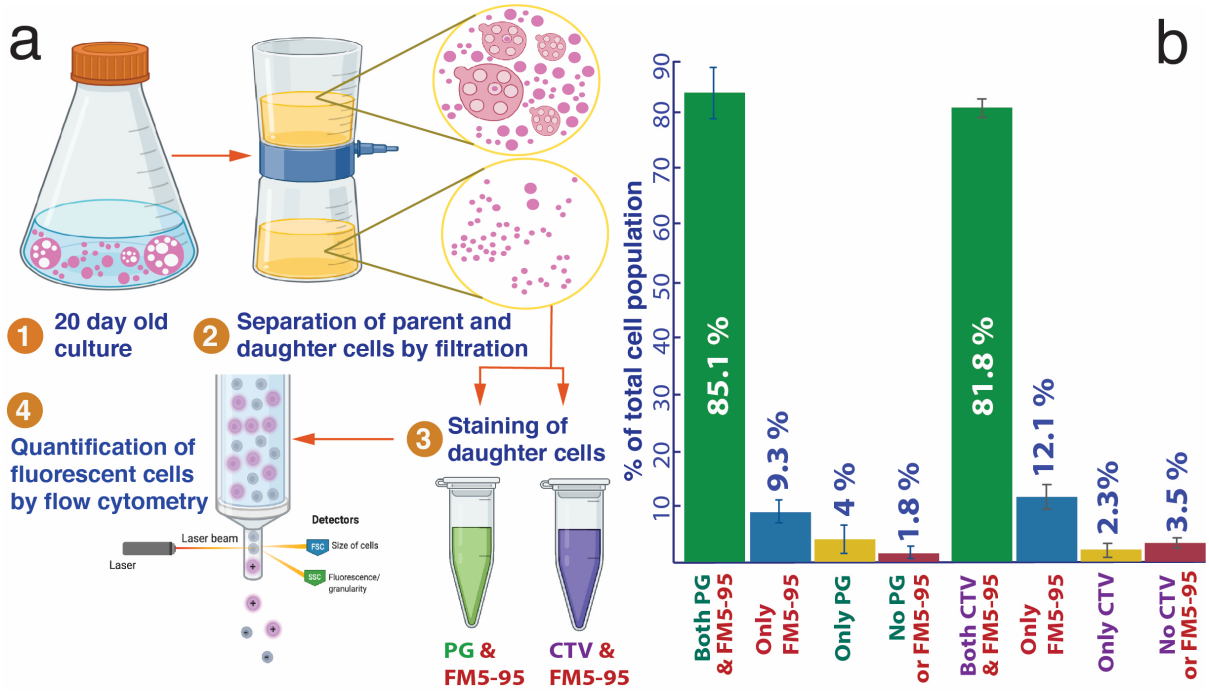

Figure 8. Presence of DNA and cytoplasmic activity in *EM-P* daughter cells. Panel-a shows the workflow of the experiment. Image-b shows the percentage of *EM-P* daughter cells that received DNA from the parent cell and possess cytoplasmic activity as determined by staining the cells with FM™5-95 (FM5, cell membrane), PicoGreen™ (PG, DNA), and CellTrace™ Violet (CTV, cytoplasmic activity). The relative percentages of cells stained with individual, and combinations of these dyes were quantified by flow cytometry. The original flow cytometry plots together with the confocal microscope images of daughter cells were shown in Figure S12 & S13.

The efficiency of reproduction in *EM-P* was also dependent on the environmental conditions, under which cells were grown. Less leakage of cell constituents was observed when cells were grown in the presence of $MgCl_2$, compared to other salts (Figure 7 & S9). Significantly less leakage of cell constituents was also observed when *EM-P* was grown on an orbital shaker than under static conditions (Figure 7 & S9). These observations suggest that the reproductive efficiency of *EM-P*-like cells could be higher in natural environments than what

was observed in our static incubations. Despite the low reproductive efficiency, *EM-P* batch cultures always resulted in viable daughter cells (Figure 8). Staining and quantification of cells by flow cytometry showed that most daughter cells received DNA from the parent cell and exhibited cytoplasmic activity (Figure 8). Moreover, inoculation of smaller daughter cells after passing through 0.44μm filter to separate them from membrane debris and other larger cells always resulted in growth.

EM-P exhibited considerable cell-to-cell variations in its size, number/size of intracellular vesicles, and the length of filamentous extensions. Similar unpredictability in morphologies was reported earlier in LVs in the elongational flow path[52,53]. Recent studies focused on the understanding this chaotic behavior, concluded that infinitesimal perturbation on the surface of LVs could have a disproportionate effect on their end morphology. LVs with ever-changing aspect ratios resulted in an unpredictable mix of end morphologies. *EM-P* cells in their exponential growth stage resemble LVs undergoing expansion strain. Cell-to-cell variations in its morphologies could be explained by small differences in the initial aspect rations of individual cells, especially given the complex lipid, protein compositions of cell membranes[36] and spontaneous curvatures heterogenicities[24]. As mentioned before, apart from the infinitesimal perturbation that arise due differences in lipid composition, *EM-P* also exhibited visible membrane undulations *i.e.,* aspect ratio fluctuations (constant deformations at the cell surface) (Movie S1-S3 & S9-S12). Hence, we propose this ever-changing aspect ratio could also have contributed to cell-to-cell variations observed in their morphology.

To the best of our knowledge, ours is the first study to demonstrate reproduction of model protocell in their natural habitat. The process of reproduction we described here closely resembles to the reproductive process reported from minimal cells that were a result of top-

down synthetic biology approach[54] (Figure S14 & S15) and mathematical simulations of protocell reproduction process[55] (Figure S16). Like *EM-P*, both these approaches resulted in cells that reproduce either by asymmetric cell division (Figure S14b & S16b) or by forming a string of daughter cells (Figure S14b) and exhibit the formation of hollow intracellular vesicles (Figure S15a). Nevertheless, our proposal that protocell reproduced by these processes is predicated on three key presumptions. First, early Earth's oceans should have salt content of 5-10% w/v, similar to the growth conditions employed in our study. These conditions are required for maintaining a state of osmotic non-equilibrium between the cell and its surrounding[12,45], which in-turn is necessary to keep cells in a constant state of shape fluctuations. We argue that such surface undulations could have played an important role in the mediating cell-division (Movie S1-S3 & S9-S11). Second, the membranes of these protocells should have been of complex phospholipid composition. An osmotic non-equilibrium with the surrounding can only be only be maintained for a prolonged period, if the membrane is composed of phospholipids rather than considerably more permeable fatty acid[4]. Cell membranes of complex phospholipid composition are also necessary to resist precipitation or crystallization of phospholipids and to establish a lateral heterogenicity[56,57], which is required for budding and ultimate formation of daughter cells. Third, given the impermeability of phospholipid membranes to polar compounds, by the time the above-described processes became prevalent, protocells already should have evolved metabolic pathways for conservation of energy and biochemical processes for synthesis of cell constituents[4], rather than passively taking up pre-reduced organic carbon from the surroundings. For these reasons, we believe that protocells reproducing by above-described processes represent an evolutionarily a more advanced (*i.e.,* late) state of protocells. Inferences from geological, paleontological, and environmental studies of early Earth are in agreement with all three prerequisites.

Paleontological evidence suggests that life in the Archaean Eon was exclusively restricted to costal marine environments[49-52]. Cells inhabiting these environments likely experienced a range of salinities used in our experiments, due to concentration of salt by evaporation of sea water in the tidal zones[58] or due to the higher salinities of the Archaean oceans[20]. In support of this presumption, earliest known microfossils were closely associated with salt crystals[59] and were enclosed in clasts of organic carbon exhibiting desiccation cracks - a geological indicator for high concentration of salt in these sites. Apart from our study, significance for higher salinities for the origin of life was also proposed by other studies[58]. Although in theory, environmental conditions of early Earth seems to be conducive for the above described processes to happen[20], arguing that protocells possessed an internal metabolism and that their membranes were composed of diverse phospholipids, first requires us to provide an empirical evidence for the existence of such cells on early Earth. Unlike other theories on evolution, existence of protocells has not been proven empirically. Hence, we looked into the geological record of the earliest known evidence of life for the existence of fossilized cells that were morphologically similar to the one from our study. Cells from our study bares remarkable morphological similarity with earliest known microfossils. Similar to what was observed in our study fossilized cells exhibited large intracellular vacuoles and internal daughter cells[60]. Extensive morphological comparison of microfossils with that of cells from our study, showed beyond a reasonable doubt that cells reproducing by the processes we described here, indeed existed on early Earth[60]. Moreover, elemental and isotopic signature of these microfossils suggest that these fossilized cells were metabolically active[15,61]. Spatial differences in the carbon isotope composition in these fossilized cells suggest that their cell membranes exhibited lateral heterogenicities[62,60]. Given these similarities between our results and microfossils, both of which being in agreement with that of top-down[54] and

computational approaches[55], we propose that protocells reproduced by a process similar to what we described here.

In conclusion, our work alters the current presumption that molecular biological processes are necessary for mediating complex biological processes like reproduction. Our results suggest that reproduction is an innate biophysical property of cells that possess an internal metabolism. In the absence of molecular biological processes, cells reproduced rather in-efficiently with a considerable loss of intracellular contents. Nevertheless, efficiency of reproduction is dependent on the environmental conditions. Given the simplicity and robustness of the process under environmental conditions of early Earth, we propose that proto-Gram-positive bacteria reproduced by these processes. In short, we present a method by which protocells reproduced prior to the evolution of molecular biological processes.

Methods

Exiguobacterium strain-M was isolated from submerged biofilms in the Dead Sea[63]. This isolate was chosen because of its ability to grow in different types of salts (NaCl, KCl, $MgCl_2$ & Dead Sea salt) and concentrations up to 10% w/v.

Protoplasts of *Exiguobacterium* Strain-M (*EM-P*) were generated from by inoculating overnight cultures into half strength tryptic soya broth (TSB) containing 5% Dead Sea Salt (5%DSS-TSB), 80 µg/ml lysozyme and 200µg/ml penicillin G (all reagents were obtained from Sigma Aldrich, Germany). Transformation to protoplast was confirmed by change in cell morphology. Over the next 3-4 weeks the cells were repeatedly sub-cultured into fresh media with penicillin G and lysozyme as described above. The stability of these protoplasts

was determined after ten sub-cultures by transferring cells to their respective media without penicillin G or lysozyme. As *EM-P* did not revert to their native morphology under salt stress, use of both Lysozyme and penicillin G was discontinued for subsequent experiments. For subsequent experiments both bacteria are grown in the media for the respective experiments described in the text.

Morphology of both *EM-P* under different growth conditions was determined using Carl Zeiss Axioskop 2plus microscope equipped with Axiocam HRm (Carl Zeiss, Germany) or Leica DSF9000 (Leica, Germany) cameras. TEM was carried out using a Zeiss EM 912 with an integrated OMEGA-filter as described before [64]. Scanning electron microscopy of *EM-P* cells was done using Versa 3D dual beam SEM microscope as described before [65].

STED microscopy was performed with an inverted TCS SP8 STED 3X microscope (Leica Microsystems, Mannheim Germany) using 86x/1.2 NA water immersion objective (Leica HC PL APO CS2 - STED White). Fluorophores were excited with either 488, 561nm, 594nm or 633m laser light derived from 80 MHz pulsed white light laser (Leica Microsystems, Mannheim Germany). For stimulated emission depletion, either a pulsed 775 nm laser or a 592nm CW laser (Leica Microsystems, Mannheim Germany) was used depended on the fluorophore. The emitted fluorescence light was collected with Hybrid Detectors (HyD, Leica Microsystems, Mannheim Germany) using appropriate emission band pass-filter setting and typically a gate of 0.3ns-6.0ns for depletion with the 775nm laser or 1.0-6.0ns with the 592nm laser. Images were recorded in photon counting mode and line accumulation. Image deconvolution was performed on selected images and movies with Huygens Professional (version 16.10.1p2, Scientific Volume Imaging, Hilversum, The Netherlands).

Spinning Disk Microscopy was performed using an Olympus SpinSR10 spinning disk confocal microscope (Olympus, Tokyo, Japan) equipped with an 100x/NA1.35 silicone oil immersion objective (Olympus UPLSAPO100XS, Tokyo, Japan), a CSU-W1-Spinning Disk-Unit (Yokogawa, Tokyo, Japan) and ORCA-Flash 4.0 V3 Digital CMOS Camera (Hamamatsu, Hamamatsu City, Japan).

Quantification of extracellular and intracellular DNA was done as follows. *EM-P* was inoculated into respective media with different types of salts. The culture bottles were either incubated under static conditions or on an orbital shaker at 160 rpm. 2ml of cells were harvested every 24h time intervals from all the incubations. In case of static cultures, incubations were placed on an orbital shaker for 20 min at 80 rpm to disperse the biofilm. Intact cells were precipitated by centrifugation at 6000 rpm for 10 min. DNA was extracted from both cell and supernatant using phenol-chloroform extraction. In the final step, DNA was washed with 70% ethanol for three times to remove salts from DNA. The resultant DNA was dissolved in 0.2 ml of TE buffer. Quantification of DNA was done using Qubit dsDNA quantification kit (Invitrogen).

Viability of daughter cells was determined by growth of daughter cells either by directly sub-culturing 10-20 day old cultures into fresh media or by passing 10-20 day old cultures through 0.45µm cellulose acetate filter and then transferring the filtrate into fresh media. Cytoplasmic activity in daughter cells was also tested by staining them with DNA stain, PicoGreen™ and live cell labelling CellTrace™ violet stain (Invitrogen) and imaging the cells under a point scanning confocal microscope.

To understand the relative contribution of intracellular processes and asymmetric conditions on either side of the cell membrane on surface oscillations, we treated cells with 2% methanol-free

formaldehyde (ThermoFisher)[29] to polymerize and inactivate the movement of proteins inside the cell. Cells were also treated with 0.3% sodium azide[28]. Minimum inhibitory concentrations of soidum azide to *RS-P* was predetermined by exposing cells to sodium azide concentrations from 0.1 to 1% w/v for 4 hours. Subsequent transfer of these cells exposed to sodium azide (0.3%)[28] did not result in growth. To equilibrate the conditions in and out of the cells Cells were permeabilized using 0.5% Triton X-100 (Sigma)[29] for 40 min and subsequently rinsed twice with growth media.

Acknowledgments: We gratefully acknowledge Ralf Conrad and Petra Schwille for their input throughout the work. We would like to thank Gabriella Berthal and Markus Oster for excellent technical support. We would also like to thank Advanced Light Microscopy Facility at EMBL, Heidelberg, Ulf Schwartz from Leica Microsystems and other members of Ecological microbiology laboratory for their support throughout the work. We thank Petra Schwille for critical reading of the manuscript. This research was funded by the European Research Council (ERC), grant agreement 616644 (POLLOX) to TL, DFG-TRR174 to PS and Origins Excellence Cluster seed money to DK.

Author contributions: DK conceived the work with input from ML, FH, TB, AK, PP, JHK & TL. DK performed laboratory experiments. DK & ML performed confocal and super-resolution imaging. AK did TEM imaging. DK coordinated work between the authors. DK wrote the manuscript with input from ML, TL & JHK.

Declaration of interests: The authors declare no competing interests.

References

(1) Oparin, A. I. Chemistry and the Origin of Life. *R. Inst. Chem. Rev.* **1969**, *2*, 1-12.

(2) Zhu, T. F.; Szostak, J. W. Coupled Growth and Division of Model Protocell Membranes. *J. Am. Chem. Soc.* **2009**, *131*, 5705-5713.

(3) Hanczyc, M. M.; Fujikawa, S. M.; Szostak, J. W. Experimental Models of Primitive Cellular Compartments: Encapsulation, Growth, and Division. *Science.* **2003**, *302*, 618–622.

(4) Budin, I.; Szostak, J. W. Physical Effects Underlying the Transition from Primitive to Modern Cell Membranes. *Proc. Natl. Acad. Sci.* **2011**, *108*, 5249–5254.

(5) van Heijenoort, J. Lipid Intermediates in the Biosynthesis of Bacterial Peptidoglycan. *Microbiol. Mol. Biol. Rev.* **2007**, *71, 620*–635.

(6) Bouhss, A.; Trunkfield, A. E.; Bugg, T. D. H.; Mengin-Lecreulx, D. The Biosynthesis of Peptidoglycan Lipid-Linked Intermediates. *FEMS Microbiology Reviews*. **2008**. *32*, 203–233.

(7) Leaver, M.; Dominguez-Cuevas, P.; Coxhead, J. M.; Daniel, R. A.; Errington, J. Life without a Wall or Division Machine in Bacillus Subtilis. *Nature* **2009**, *457*, 849-853.

(8) Mercier, R.; Kawai, Y.; Errington, J. Excess Membrane Synthesis Drives a Primitive Mode of Cell Proliferation. *Cell,* **2013**, *152*, 997–1007.

(9) Errington, J. L-Form Bacteria, Cell Walls and the Origins of Life. *Open Biol.* **2013**, *3*, 120143.

(10) Wu, L. J.; Lee, S.; Park, S.; Eland, L. E.; Wipat, A.; Holden, S.; Errington, J. Geometric Principles Underlying the Proliferation of a Model Cell System. *Nat. Commun.* **2020**, *11,* 4149.

(11) Tsai, H. H. G.; Lai, W. X.; Lin, H. Da; Lee, J. Bin; Juang, W. F.; Tseng, W. H. Molecular Dynamics Simulation of Cation-Phospholipid Clustering in Phospholipid

Bilayers: Possible Role in Stalk Formation during Membrane Fusion. *Biochim. Biophys. Acta - Biomembr.* **2012**, *1818*, 2742-2755.

(12) Karimi, M.; Steinkühler, J.; Roy, D.; Dasgupta, R.; Lipowsky, R.; Dimova, R. Asymmetric Ionic Conditions Generate Large Membrane Curvatures. *Nano Lett.* **2018**, *18*, 7816-7821.

(13) Mojzsis, S. J.; Harrison, T. M.; Pidgeon, R. T. Oxygen-Isotope Evidence from Ancient Zircons for Liquid Water at the Earth's Surface 4,300 Myr Ago. *Nature* **2001**, *409,* 178-181.

(14) Mojzsis, S. J.; Arrhenius, G.; McKeegan, K. D.; Harrison, T. M.; Nutman, A. P.; Friend, C. R. L. Evidence for Life on Earth before 3,800 Million Years Ago. *Nature* **1996**, *384*, 55-59.

(15) Dodd, M. S.; Papineau, D.; Grenne, T.; Slack, J. F.; Rittner, M.; Pirajno, F.; O'Neil, J.; Little, C. T. S. Evidence for Early Life in Earth's Oldest Hydrothermal Vent Precipitates. *Nature* **2017**, *543*, 60–64.

(16) Schopf, J. W. Microfossils of the Early Archean Apex Chert: New Evidence of the Antiquity of Life. *Science.* **1993**, *260*, 640–646.

(17) Põldsalu, I.; Koksal, E. S.; Friis, H.; Mojzsis, S.; Bizzarro, M.; Gozen, I. Spontaneous Formation of Prebiotic Compartment Colonies on Hadean Earth and Pre-Noachian Mars. *Biophys. J.* **2022**, *121*, e202100040.

(18) Blake, R. E.; Chang, S. J.; Lepland, A. Phosphate Oxygen Isotopic Evidence for a Temperate and Biologically Active Archaean Ocean. *Nature* **2010**, *464*, 1029–1032.

(19) Catling, D. C.; Zahnle, K. J. The Archean Atmosphere. *Sci. Adv.* **2020**, *6*, eaax1420.

(20) Knauth, L. P. Salinity History of the Earth's Early Ocean. *Nature* **1998**, *395*, 554.

(21) Derényi, I.; Lagzi, I. Fatty Acid Droplet Self-Division Driven by a Chemical Reaction. *Phys. Chem. Chem. Phys.* **2014**, *16*, 4639–4641.

(22) Zwicker, D.; Seyboldt, R.; Weber, C. A.; Hyman, A. A.; Jülicher, F. Growth and Division of Active Droplets Provides a Model for Protocells. *Nat. Phys.* **2017**, *13*, 408-413.

(23) Kurihara, K.; Tamura, M.; Shohda, K. I.; Toyota, T.; Suzuki, K.; Sugawara, T. Self-Reproduction of Supramolecular Giant Vesicles Combined with the Amplification of Encapsulated DNA. *Nat. Chem.* **2011**, *3*, 775-781.

(24) Bobrovska, N.; Góźdź, W.; Kralj-Iglič, V.; Iglič, A. On the Role of Anisotropy of Membrane Components in Formation and Stabilization of Tubular Structures in Multicomponent Membranes. *PLoS One.* **2013**, 8, e73941.

(25) Simons, K.; Ikonen, E. Functional Rafts in Cell Membranes. *Nature*. **1997**. *387*, 569-572.

(26) Corradi, V.; Sejdiu, B. I.; Mesa-Galloso, H.; Abdizadeh, H.; Noskov, S. Y.; Marrink, S. J.; Tieleman, D. P. Emerging Diversity in Lipid-Protein Interactions. *Chemical Reviews*. **2019**, *119*, 5775-5848.

(27) Kawai, Y.; Mercier, R.; Wu, L. J.; Domínguez-Cuevas, P.; Oshima, T.; Errington, J. Cell Growth of Wall-Free L-Form Bacteria Is Limited by Oxidative Damage. *Curr. Biol.* **2015**, *25*, 1613–1618.

(28) Yanagisawa, M.; Imai, M.; Taniguchi, T. Shape Deformation of Ternary Vesicles Coupled with Phase Separation. *Phys. Rev. Lett.* **2008**, *100*, 148102-4.

(29) Yanagisawa, M.; Imai, M.; Taniguchi, T. Periodic Modulation of Tubular Vesicles Induced by Phase Separation. *Phys. Rev. E - Stat. Nonlinear, Soft Matter Phys.* **2010**, *82*, 051928-1-9.

(30) Liu, Y.; Agudo-Canalejo, J.; Grafmüller, A.; Dimova, R.; Lipowsky, R. Patterns of Flexible Nanotubes Formed by Liquid-Ordered and Liquid-Disordered Membranes. *ACS Nano* **2016**. *10*, 463-474.

(31) Lipowsky, R. Budding of Membranes Induced by Intramembrane Domains. *J. Phys. II* **1992**, *2*, 1825-1840.

(32) Jülicher, F.; Lipowsky, R. Domain-Induced Budding of Vesicles. *Phys. Rev. Lett.* **1993**, *70*, 2964.

(33) Sáenz, J. P.; Grosser, D.; Bradley, A. S.; Lagny, T. J.; Lavrynenko, O.; Broda, M.; Simons, K. Hopanoids as Functional Analogues of Cholesterol in Bacterial Membranes. *Proc. Natl. Acad. Sci. U. S. A.* **2015**. *112*, 11971-11976.

(34) Baumgart, T.; Hess, S. T.; Webb, W. W. Imaging Coexisting Fluid Domains in Biomembrane Models Coupling Curvature and Line Tension. *Nature* **2003**, *425*, 821-824.

(35) Bacia, K.; Schwille, P.; Kurzchalia, T. Sterol Structure Determines the Separation of Phases and the Curvature of the Liquid-Ordered Phase in Model Membranes. *Proc. Natl. Acad. Sci. U. S. A.* **2005**. *102*, 3272-3277.

(36) Sáenz, J. P.; Grosser, D.; Bradley, A. S.; Lagny, T. J.; Lavrynenko, O.; Broda, M.; Simons, K. Hopanoids as Functional Analogues of Cholesterol in Bacterial Membranes. *Proc. Natl. Acad. Sci. U. S. A.* **2015**. *112*, 11971-11976.

(37) Andes-Koback, M.; Keating, C. D. Complete Budding and Asymmetric Division of Primitive Model Cells to Produce Daughter Vesicles with Different Interior and Membrane Compositions. *J. Am. Chem. Soc.* **2011**, *133*, 9545-9555.

(38) Li, Y.; Lipowsky, R.; Dimova, R. Membrane Nanotubes Induced by Aqueous Phase Separation and Stabilized by Spontaneous Curvature. *Proc. Natl. Acad. Sci. U. S. A.* **2011**. *108*, 4731-4736.

(39) Sanborn, J.; Oglęcka, K.; Kraut, R. S.; Parikh, A. N. Transient Pearling and Vesiculation of Membrane Tubes under Osmotic Gradients. *Faraday Discuss.* **2012**, *161*, 167-176.

(40) Pelletier, J. F.; Sun, L.; Wise, K. S.; Assad-Garcia, N.; Karas, B. J.; Deerinck, T. J.; Ellisman, M. H.; Mershin, A.; Gershenfeld, N.; Chuang, R. Y.; Glass, J. I.; Strychalski, E. A. Genetic Requirements for Cell Division in a Genomically Minimal Cell. *Cell* **2021**, *184*, 2430-2440.

(41) Olivi, L.; Berger, M.; Creyghton, R. N. P.; De Franceschi, N.; Dekker, C.; Mulder, B. M.; Claassens, N. J.; ten Wolde, P. R.; van der Oost, J. Towards a Synthetic Cell Cycle. *Nat. Commun.* **2021**, *12*, Article number 4531.

(42) Schwille, P. Division in Synthetic Cells. *Emerg. Top. Life Sci.* **2019**, 3, 551-558.

(43) Deshpande, S.; Spoelstra, W. K.; Van Doorn, M.; Kerssemakers, J.; Dekker, C. Mechanical Division of Cell-Sized Liposomes. *ACS Nano* **2018**, *12,* 2560–2568.

(44) Litschel, T.; Ramm, B.; Maas, R.; Heymann, M.; Schwille, P. Beating Vesicles: Encapsulated Protein Oscillations Cause Dynamic Membrane Deformations. *Angew. Chemie - Int. Ed.* **2018**, *57*, 16286-16290.

(45) Oglęcka, K.; Rangamani, P.; Liedberg, B.; Kraut, R. S.; Parikh, A. N. Oscillatory Phase Separation in Giant Lipid Vesicles Induced by Transmembrane Osmotic Differentials. *Elife* **2014**, *3*, e03695.

(46) Levy, S.; Chevion, M. Synergistic Cytotoxic Effect of Tetrachlorocatechol and Sodium Azide in Escherichia Coli: Toxicity, Metabolism, and Mechanistic Aspects. *Environ. Toxicol. Chem.* **2009**, *28*, 1380-1389.

(47) Spahn, C.; Grimm, J. B.; Lavis, L. D.; Lampe, M.; Heilemann, M. Whole-Cell, 3D, and Multicolor STED Imaging with Exchangeable Fluorophores. *Nano Lett.* **2019**, *19*, 500-505.

(48) Vutukuri, H. R.; Hoore, M.; Abaurrea-Velasco, C.; van Buren, L.; Dutto, A.; Auth, T.; Fedosov, D. A.; Gompper, G.; Vermant, J. Active Particles Induce Large Shape Deformations in Giant Lipid Vesicles. *Nature* **2020**, **2020**, *586*, 52-56.

(49) Blöchliger, E.; Blocher, M.; Walde, P.; Luisi, P. L. Matrix Effect in the Size Distribution of Fatty Acid Vesicles. *J. Phys. Chem. B* **1998**, *102*, 10383–10390.

(50) Zhu, T. F.; Szostak, J. W. Exploding Vesicles. *J. Syst. Chem.* **2011**, *2*, Article number 4.

(51) Angelova, M. I.; Hristova, N.; Tsoneva, I. DNA-Induced Endocytosis upon Local Microinjection to Giant Unilamellar Cationic Vesicles. *Eur. Biophys. J.* **1999**, *28*, 142–150.

(52) Kantsler, V.; Segre, E.; Steinberg, V. Critical Dynamics of Vesicle Stretching Transition in Elongational Flow. *Phys. Rev. Lett.* **2008**. 048101.

(53) Narsimhan, V.; Spann, A. P.; Shaqfeh, E. S. G. The Mechanism of Shape Instability for a Vesicle in Extensional Flow. *J. Fluid Mech.* **2014**, *750*, 144-190.

(54) Hutchison, C. A.; Chuang, R. Y.; Noskov, V. N.; Assad-Garcia, N.; Deerinck, T. J.; Ellisman, M. H.; Gill, J.; Kannan, K.; Karas, B. J.; Ma, L.; Pelletier, J. F.; Qi, Z. Q.; Richter, R. A.; Strychalski, E. A.; Sun, L.; Suzuki, Y.; Tsvetanova, B.; Wise, K. S.; Smith, H. O.; Glass, J. I.; Merryman, C.; Gibson, D. G.; Venter, J. C. Design and Synthesis of a Minimal Bacterial Genome. *Science.* **2016**, 351, 6280.

(55) Ruiz-Herrero, T.; Fai, T. G.; Mahadevan, L. Dynamics of Growth and Form in Prebiotic Vesicles. **2019,** *arXiv Prepr. arXiv1901.04406*.

(56) Jordan, S. F.; Nee, E.; Lane, N. Isoprenoids Enhance the Stability of Fatty Acid Membranes at the Emergence of Life Potentially Leading to an Early Lipid Divide. *Interface Focus* **2019**, *9*, 20190067.

(57) Jordan, S. F.; Rammu, H.; Zheludev, I. N.; Hartley, A. M.; Maréchal, A.; Lane, N. Promotion of Protocell Self-Assembly from Mixed Amphiphiles at the Origin of Life. *Nat. Ecol. Evol.* **2019**, *3*, 1705-1714.

(58) Spitzer, J.; Poolman, B. The Role of Biomacromolecular Crowding, Ionic Strength,

and Physicochemical Gradients in the Complexities of Life's Emergence. *Microbiol. Mol. Biol. Rev.* **2009**, *73*, 371–388.

(59) Alleon, J.; Bernard, S.; Le Guillou, C.; Beyssac, O.; Sugitani, K.; Robert, F. Chemical Nature of the 3.4 Ga Strelley Pool Microfossils. *Geochemical Perspect. Lett.* **2018**, *7*, 37–42.

(60) Kanaparthi, D.; Lampe, M.; Zhu, B.; Boesen, T.; Klingl, A.; Schwille, P.; Lueders, T. On the Nature of the Earliest Known Lifeforms. *bioRxiv* **2021**, 2021.08.16.456462.

(61) Wacey, D.; Kilburn, M. R.; Saunders, M.; Cliff, J.; Brasier, M. D. Microfossils of Sulphur-Metabolizing Cells in 3.4-Billion-Year-Old Rocks of Western Australia. *Nat. Geosci.* **2011**, *4*, 698–702.

(62) Lepot, K.; Williford, K. H.; Ushikubo, T.; Sugitani, K.; Mimura, K.; Spicuzza, M. J.; Valley, J. W. Texture-Specific Isotopic Compositions in 3.4 Gyr Old Organic Matter Support Selective Preservation in Cell-like Structures. *Geochim. Cosmochim. Acta* **2013**, *112*, 66–86.

(63) Häusler, S.; Noriega-Ortega, B. E.; Polerecky, L.; Meyer, V.; de Beer, D.; Ionescu, D. Microenvironments of Reduced Salinity Harbour Biofilms in Dead Sea Underwater Springs. *Environ. Microbiol. Rep.* **2014**. *6*, 152-158.

(64) Cerri, M. R.; Wang, Q.; Stolz, P.; Folgmann, J.; Frances, L.; Katzer, K.; Li, X.; Heckmann, A. B.; Wang, T. L.; Downie, J. A.; Klingl, A.; de Carvalho-Niebel, F.; Xie, F.; Parniske, M. The ERN1 Transcription Factor Gene Is a Target of the CCaMK/CYCLOPS Complex and Controls Rhizobial Infection in Lotus Japonicus. *New Phytol.* **2017**, *215*, 323-337.

(65) Cornelissen, R.; Bøggild, A.; Thiruvallur Eachambadi, R.; Koning, R. I.; Kremer, A.; Hidalgo-Martinez, S.; Zetsche, E.-M.; Damgaard, L. R.; Bonné, R.; Drijkoningen, J.; Geelhoed, J. S.; Boesen, T.; Boschker, H. T. S.; Valcke, R.; Nielsen, L. P.; D'Haen, J.;

Manca, J. V.; Meysman, F. J. R. The Cell Envelope Structure of Cable Bacteria. *Front. Microbiol.* **2018**, *9*. 3044.

Supporting information: Supplemental figures (Figure S1-S16) and supplementary movies (Movie S1-22).